

Superrevivals in the quantum dynamics of a particle confined in a finite square well potential

Anu Venugopalan[†] and G. S. Agarwal[‡]
*Physical Research Laboratory, Navrangpura
 Ahmedabad, , INDIA -380 009*

We examine the revival features in wave packet dynamics of a particle confined in a finite square well potential. The possibility of tunneling modifies the revival pattern as compared to an infinite square well potential. We study the dependence of the revival times on the depth of the square well and predict the existence of superrevivals. The nature of these superrevivals is compared with similar features seen in the dynamics of wavepackets in an anharmonic oscillator potential.

42.50. Md, 03.65. Ge, 03.65. -w

I. INTRODUCTION

The wavepacket in quantum mechanics is often viewed as the most ‘nearly classical’ state and is known to exhibit many striking classical properties. However, its inherent quantum nature also causes it to exhibit many quantum mechanical features. It is known [1,2] that in certain nonlinear quantum systems the dynamics of the wave packet incorporates quantum interference effects which cause it to undergo a sequence of collapses and revivals and in the course of its evolution the wavepacket periodically breaks up and reconstitutes its original form. At intermediate times the wavepacket gathers into a series of subsidiary wavepackets called fractional revivals [3]. Quantum revivals are often a manifestation of the fact that the time evolution of the wavepacket is driven by a discrete eigenvalue spectrum and revival features depend on the way the eigenenergies of the quantum system depend on the quantum number, n [3,4]. Recently there has been a lot of interest in the theoretical and experimental study of quantum revivals in a variety of nonlinear systems like that of Rydberg atom wavepackets [2], molecular wavepackets [5], wave packets in semiconductor quantum wells [6] etc. Most experiments dealing with quantum revivals till date focus on atomic [2] and molecular systems [5], photon cavity systems [7] and ions in traps [8]. The simplest class of systems for which one would see fractional and full revivals are those for which the energy spectrum goes as n^2 , e.g., the infinite square well potential and the rigid rotator [4]. For systems with a nonquadratic dependence on n , one can see a new sequence of collapse and revivals which are different from the usual fractional revivals. Often these sequences culminate with the wavepacket resembling its original form more closely. These are superrevivals [4,9]. The revival patterns of Rydberg wavepackets, where the energy spectrum is nonquadratic in n , have been seen to exhibit such superrevivals [9].

An ideal model system to illustrate the fractional revival phenomenon is the infinite square well potential since simple analytical forms of the eigenvalues and the

eigenfunctions allow for an easy analysis of the time evolution of any initial state. This system has been recently studied in great detail in the context of fractional revivals [10,11] as well as for the space-time structures [12] that appear in the dynamical evolution. An experimental realization of the predictions of the fractional revival phenomenon in the infinite well is most likely to be in semiconductor quantum well systems. In reality, however, it is rather impossible to find a physical system that creates a truly infinite confining potential. It becomes crucial, therefore, to study the problem of revivals in more realistic, *physical* systems which are better described by finite well potentials rather than infinite potentials. The possibility of the occurrence of both revivals and superrevivals in a finite potential well has been pointed out before [10] though no explicit study has been done till now. From a more fundamental point of view, the motivation to study the finite well system is to get a greater insight into understanding the ‘classical limit’. During the course of its evolution an initially localized wavepacket appears at certain times as a linear superposition of spatially separated copies of itself, i.e., in Schrödinger cat-like states. The tremendous progress in experiments involving semiconductor systems, e.g, the observation of quantum beats in quantum wells [6] and Bloch oscillations in semiconductor superlattices [13] increases the prospects of generating, detecting and studying such cat-like states among other features like revivals, thus providing further motivations to get a better theoretical understanding of these systems.

In this paper we focus on the revival features of wavepackets in *finite* square well potentials and compare it with the corresponding case for the infinite well. For our purpose we have only concerned ourselves with the bound eigenstates of the finite square well potential. According to quantum mechanics, the wavefunction has nonvanishing values in the classically forbidden regions thus giving a nonvanishing probability for the particle being outside the well. One thus expects a difference in the wavepacket dynamics as compared to the infinite well case. We show that the existence of the possibil-

ity of tunneling modifies the revival pattern as compared to the infinite square well potential. In particular it allows for revivals *and* superrevivals. We show that usual revival times are now longer compared to that of the infinite well and depend on the well depth. The paper is organized as follows. In Section II we begin by introducing the concept of fractional revivals and review briefly the finite well problem. We then present our numerical results and confirm the approximate formula of Barker *et al.* [14] from which we deduce an approximate analytical expression for revival times in finite square well potentials. In Section III we present another key result of this paper which is the existence of superrevivals during the time evolution of an initial Gaussian wavepacket. The absence of an exact analytical expression for the energy spectrum for the finite potential well makes it difficult to give an estimate of the superrevival times. However, we get some insight into the nature of superrevivals in the well by comparing it with superrevivals in the dynamics of Gaussian wavepackets in an anharmonic oscillator potential for which we have the analytical results. Finally, we summarize our results in Section IV.

II. DEPENDENCE OF REVIVAL TIMES ON WELL-STRENGTH

Consider the time evolution of a particle initially in state $\psi(x, 0)$ in a potential:

$$\psi(x, t) = \sum_n c_n \phi_n(x) e^{-iE_n t/\hbar}, \quad (1)$$

where n is the quantum number and $\phi_n(x)$ and E_n are the energy eigenstates and corresponding eigenvalues. The coefficients c_n are given in terms of the initial wavefunction by $c_n = \langle \phi_n(x) | \psi(x, 0) \rangle$. In general the superposition (1) may also contain continuum states for which n would be a continuous index and the sum would be replaced by an integral. Here, however, we concern ourselves with only superpositions of bound states assuming negligible continuum contributions. Also, one assumes that the expansion (1) is strongly weighted around a mean value, \bar{n} . Both the assumptions above are reasonable in, e.g., the experimental situation when a localized wavepacket is produced using a short laser pulse [1]. If one assumes that the weighting probabilities $|c_n|^2$ are strongly centered around a mean value \bar{n} , one can expand the energy in a Taylor series in n around \bar{n} as:

$$E_n = E_{\bar{n}} + E'_{\bar{n}}(n - \bar{n}) + \frac{1}{2}E''_{\bar{n}}(n - \bar{n})^2 + \frac{1}{6}E'''_{\bar{n}}(n - \bar{n})^3 + \dots \quad (2)$$

where the primes denote derivatives with respect to n . From (2) one can identify the time scales,

$$T_{cl} = \frac{2\pi\hbar}{|E'_{\bar{n}}|}, \quad T_{rv} = \frac{2\pi\hbar}{\frac{1}{2}|E''_{\bar{n}}|}, \quad T_{sr} = \frac{2\pi\hbar}{\frac{1}{6}|E'''_{\bar{n}}|}, \dots \quad (3)$$

etc. which are generally termed in the literature as the classical, revival, superrevival times and so on [4]. One can easily see that re-writing the time evolution (1) in terms of these time scales shows how they govern the time evolution of $\psi(x, 0)$. The time scales in turn are controlled by the dependence of the energy on the quantum number n . For the simple case of the infinite well, the quantized energy levels are exactly quadratic in n :

$$E_n = \frac{\pi^2 \hbar^2 n^2}{2mL^2}, \quad (4)$$

where m is the mass of the particle and L is the length of the well. Corresponding to this, one has the time scales $T_{cl} = 2mL^2/\pi\hbar\bar{n}$, $T_{rv} = 4mL^2/\pi\hbar$ while $T_{sr} = \infty$. The time evolution (1) can be re-written as:

$$\psi(x, t) = \sum_n c_n \phi_n(x) e^{-2\pi i(t/T_{rv})n^2}. \quad (5)$$

The expansion (5) includes both odd and even parity states. It is easy to see that the wavefunction regains its original form i.e., shows full revivals, whenever t equals some multiple of T_{rv} , and shows fractional revivals whenever t is equal to some rational fraction of T_{rv} , e.g., $T_{rv}/4$, but no higher order effects like superrevivals are seen in the dynamics of the wavepacket for the infinite square well potential [10].

We now turn to the problem of the finite square well potential which is the focus of this paper. The one-dimensional finite square well potential for a well of length L can be described as:

$$\begin{aligned} V(x) &= 0, & |x| &\leq \frac{L}{2} \\ V(x) &= V_0, & |x| &> \frac{L}{2}. \end{aligned} \quad (6)$$

The system thus has three distinct regions and the solutions to the Schrödinger equation gives us the energy eigenstates and eigenvalues. The even parity solutions for the three regions are:

$$\begin{aligned} \phi_I(\bar{x}) &= A e^{\beta_n} \cos \alpha_n e^{2\beta_n \bar{x}}, \\ \phi_{II}(\bar{x}) &= A \cos 2\alpha_n \bar{x}, \\ \phi_{III}(\bar{x}) &= A e^{\beta_n} \cos \alpha_n e^{-2\beta_n \bar{x}}, \end{aligned} \quad (7)$$

where the eigenvalues are evaluated by solving the transcendental equation

$$\alpha_n \tan \alpha_n = \beta_n, \quad (8)$$

while the odd parity solutions are given by:

$$\begin{aligned} \phi_I(\bar{x}) &= -A e^{\beta_n} \sin \alpha_n e^{2\beta_n \bar{x}}, \\ \phi_{II}(\bar{x}) &= A \sin 2\alpha_n \bar{x}, \\ \phi_{III}(\bar{x}) &= A e^{\beta_n} \sin \alpha_n e^{-2\beta_n \bar{x}}, \end{aligned} \quad (9)$$

with eigenvalues given by the transcendental equation

$$\alpha_n \cot \alpha_n = -\beta_n. \quad (10)$$

Here $\bar{x} = x/L$ where L is the length of the square well, $\alpha_n = \sqrt{mEL^2/2\hbar^2}$ and $\beta_n = \sqrt{m(V_0 - E)L^2/2\hbar^2}$, with E the energy ($E < V_0$) and m the mass of the particle and the normalization constant A is given as:

$$A = \sqrt{\frac{2}{1 + \frac{1}{\beta_n}}}. \quad (11)$$

It is clear from (7) and (9) that the wavefunction has nonvanishing values in both the ‘classically forbidden’ regions *I* and *III*. The quantum mechanical probability for the particle to be somewhere in regions *I* and *III* is, therefore, nonvanishing. It is clear, though, that as one goes away from the boundaries, the probability density decreases rapidly to zero. Thus the particle with $E < V_0$ cannot really escape to infinitely long distances but stays ‘bound’ to the well. One can define

$$\epsilon = \sqrt{\frac{mV_0L^2}{2\hbar^2}} \quad (12)$$

as the ‘well-strength’ [14]. A finite well of well strength ϵ would contain a finite number of bound states, N , where $N \sim \frac{2\epsilon}{\pi} + 1$. The time evolution of any given initial states can be expressed in terms of these eigenstates and eigenvalues,

$$\psi(x, t) = \sum_n^N c_n \phi_n(x) \exp\left(-\frac{8i\alpha_n^2 \tau}{\pi}\right), \quad (13)$$

where $\tau = t/T_{rv}$ is the time scaled in terms of the revival time $T_{rv} = 4mL^2/\pi\hbar$ of the infinite well potential. The expansion (13) contains both odd and even parity states. For our purpose we examine the quantum dynamics of an initial Gaussian wavepacket with mean position x_0 and zero mean momentum:

$$\psi(x, 0) = B \exp\left(-\frac{(\bar{x} - x_0)^2}{2\sigma^2}\right), \quad (14)$$

where B is the normalization constant. The time evolution involves the energy eigenvalues, α_n s and the corresponding eigenfunctions which are obtained by solving the transcendental equations (8) and (10) numerically. A Gaussian wavepacket of zero mean momentum can be faithfully constructed by a superposition of these bound states (the sum of the coefficients, $\sum |c_n|^2 \approx 1$).

Our numerical simulations for the finite well show the presence of revivals in the dynamics of the initial Gaussian wavepacket (14) similar to that seen in the case of the infinite well potential for short times. The revival times, however, are in general longer than that of the infinite well and depend on the well strength (depth), ϵ , of the finite well. Barker *et al.* [14] have shown via a first order Taylor series expansion of the transcendental equations (8) and (10) for the eigenvalues that the energy

levels of a finite well of length L and well strength ϵ can be approximated as:

$$E'_n = \frac{\pi^2 \hbar^2 n^2}{2mL^2} \left(\frac{\epsilon}{1 + \epsilon}\right)^2. \quad (15)$$

One can see that this is equivalent to the energy levels for an *infinite* well but with the larger length,

$$L' = L \left(1 + \frac{1}{\epsilon}\right). \quad (16)$$

Corresponding to this approximate expression we can thus find an expression for the approximate revival time, T'_{rv} , for the finite well in terms of T_{rv} , the revival time for the infinite well:

$$T'_{rv} = T_{rv} \left(1 + \frac{1}{\epsilon}\right)^2. \quad (17)$$

The formula of Barker *et al.* is more accurate for tightly bound eigenstates (deeper wells) than for weakly bound states (shallow wells) [14]

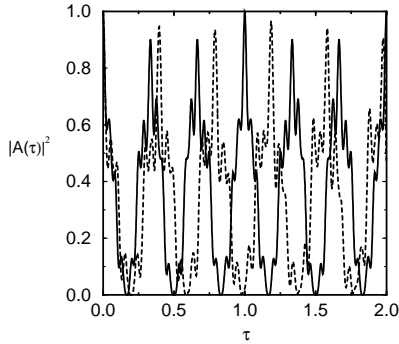
The revival features for the dynamics of any initial state can be understood by examining the absolute square of the autocorrelation function:

$$|A(\tau)|^2 = |\langle \psi(x, 0) \psi(x, \tau) \rangle|^2 = \left| \sum_n |c_n|^2 e^{-iE_n t/\hbar} \right|^2 \quad (18)$$

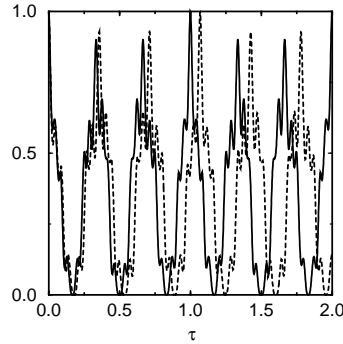
$$= \left| \sum_n |c_n|^2 e^{-8i\alpha_n^2 \tau/\pi} \right|^2.$$

Fig. 1 shows the square of the autocorrelation function, $|A(\tau)|^2$, for an initial Gaussian wavepacket for three different ‘well-strengths’, ϵ , contrasted with that for the infinite potential. One can see that for larger values of ϵ , the revival time approaches that of the infinite well ($T'_{rv} \rightarrow T_{rv}$). The agreement of the actual revival times with the formula of Barker *et al.* gets more accurate as ϵ increases, as expected and as shown in Table I. Thus for short times the dynamics of the wavepacket in the finite well is similar to that in the infinite well with modified revival times which depend on the depth of the well. For our simulations we work with the values of the parameters for the initial Gaussian state and the well-strength, ϵ such that $\sum |c_n|^2 \approx 1$ always. In Fig.1, note that the detailed behaviour of the autocorrelation function for the infinite well (solid line) shows a symmetry. In contrast, the detailed behaviour of the autocorrelation function for the finite well (dashed line) shows an asymmetry especially around the revival time as is quite evident from Fig.1(a) which corresponds to the shallowest of the three wells, ($\epsilon = 12$). As the well gets deeper, the asymmetry decreases and as expected, the detailed behaviour begins to resemble closer to the infinite well as is obvious from the ‘deeper’ well shown in Fig.1(c).

(a)



(b)



(c)

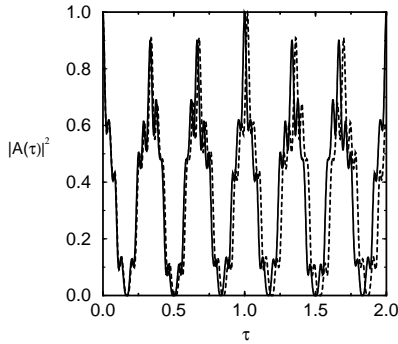


FIG. 1. Square of the autocorrelation function, $|A(\tau)|^2$ vs the scaled time τ for an initial Gaussian wavepacket of width $L/10$ centered initially at $L/5$ for the infinite well (solid-line) and finite well (dashed line) of well-strengths: (a) $\epsilon = 12(N \sim 8)$, (b) $\epsilon = 30(N \sim 20)$, (c) $\epsilon = 100(N \sim 64)$. ($\tau = t/T_{rv}, T_{rv} = 4mL^2/\pi\hbar$)

TABLE I. Comparison of the revival times, T_{rv} with the revival times estimated from the approximate formula of Barker *et al.*, T_{rvb} , for various well-strengths, ϵ . All times are scaled by $T_{rv} = 4mL^2/\pi\hbar$, the revival time for the infinite square well.

| ϵ (well-strength) | T_{rv} ($4mL^2/\pi\hbar$) | T_{rvb} ($4mL^2/\pi\hbar$) | percentage error |
|-------------------------------|----------------------------------|-----------------------------------|------------------|
| 12 ($N \sim 8$) | 1.185 | 1.174 | 0.9% |
| 30 ($N \sim 20$) | 1.06777 | 1.06876 | .09% |
| 100 ($N \sim 64$) | 1.02009 | 1.02005 | .0039 % |

III. SUPERREVIVALS

In the preceding section we examined the wavepacket dynamics and the structure of fractional revivals at short times, i.e., times of the order of or close to T'_{rv} . Now we turn to the behaviour at longer times. A look at the square of the autocorrelation function, $|A(\tau)|^2$, for longer times shows that after a few revival cycles, the wavepacket ceases to ‘reform’ faithful to its original form at $t = 0$. The peaks in $|A(\tau)|^2$ signifying full revivals go down and then pick up again after a few cycles and the wavepacket is once again closer to its original form. This new sequence of revivals is characterized by a longer revival time (T_{sr}). This behavior depends, as expected, on the depth of the finite well and is more obvious when we are dealing with shallow wells, i.e., for smaller values of ϵ . For larger depths, ϵ , the usual revivals continue for more number of cycles before the peaks in $|A(\tau)|^2$ go down and pick up again. The superrevival times, thus, get longer and longer with increase in the well depth. This is in agreement with our expectation that the behavior in a deeper finite well should approach that for the infinite well. It is interesting to note that while the usual revival times at short times decrease with increasing well-strength, ϵ , and approach that of the infinite well, $T_{rv} = 4mL^2/\pi\hbar$, the superrevival times increase with increasing ϵ approaching $T_{sr} = \infty$ for the infinite well. Since the finite well eigenenergies and eigenfunctions have no simple analytical form, it is not straightforward to estimate these superrevival times for various well-strengths ϵ . Figs. 2, 3 and 4 show the square of the autocorrelation function, $|A(\tau)|^2$, vs τ for an initial Gaussian wavepacket for two different values of the well-strength, ϵ . The structure of the plot of the square of the autocorrelation function vs the time τ is a reflection of the initial state and depends on the parameters like the width and the mean position of the initial Gaussian wavepacket. The arrow in these figures indicates the first superrevival. We have taken the case of an initial wavepacket which has its mean position at the center of the well ($x_0 = 0.0$) for Figs. 2 and 3 and ($x_0 = 0.2L$) for Fig. 4.

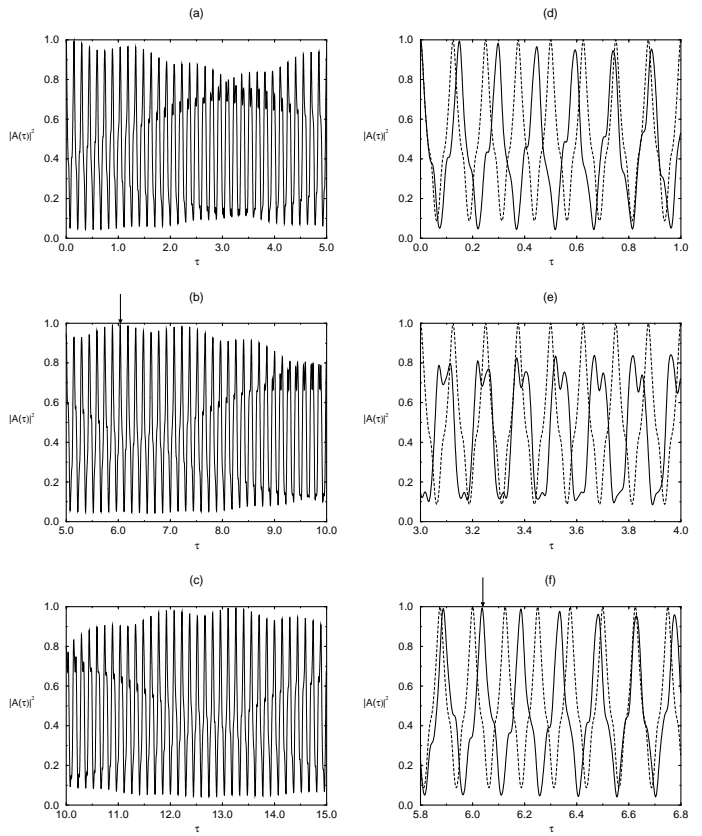


FIG. 2. Square of the autocorrelation function, $|A(\tau)|^2$ vs the scaled time τ for an initial Gaussian wavepacket of width $L/10$ and with mean position at $\bar{x} = 0.0$ for $\epsilon = 12$ ($N \sim 8$); (c) and (d) highlight the detailed behaviour at shorter times and (e) highlights the detailed behaviour near the superrevival time (e) highlights the detailed behaviour near the superrevival time (e) highlights the detailed behaviour near the superrevival time. The arrow marks the first superrevival. The dashed curves correspond to the corresponding plot for the infinite square well.

One can see that there are many revivals much before the characteristic time T'_{rv} (e.g., there are eight revivals in Fig. 2(c) and Fig. 3(c) including the one at T'_{rv}). Aronstein and Stroud [10] have pointed out this feature in their study of wavepacket dynamics in an infinite square well potential. They show that for even parity states, such as the one where the wavepacket is initially positioned at the center of the well ($x_0 = 0.0$), there are full revivals at multiples of $t = T_{rv}/8$. Similarly, odd parity states show full revivals at multiples of times $t = T_{rv}/4$. These features are obvious in the case of the dynamics in the infinite square well potential when one looks at the time evolution of an initial state in terms of the even and odd parity eigenstates:

$$\begin{aligned}\psi(\bar{x}, \tau) &= \sum_{n(\text{even})} \sqrt{2} e^{-2\pi i n^2 \tau} c_n \sin n\pi \bar{x} \\ &+ \sum_{n(\text{odd})} \sqrt{2} e^{-2\pi i n^2 \tau} c_n \cos n\pi \bar{x}.\end{aligned}\quad (19)$$

Here $\tau = t/T_{rv}$ is the scaled time and $\bar{x} = x/L$. For an initial even parity eigenstate ($\psi(\bar{x}) = \psi(-\bar{x})$), only the second summation with the cosines contributes. It can be checked that at $t = T_{rv}/8$, this sum can be written as:

$$\begin{aligned}\psi(\bar{x}, \tau) &= \sum_{n(\text{odd})} \sqrt{2} e^{-2\pi i n^2 \tau} c_n \cos n\pi \bar{x} \\ &= \sum_m \sqrt{2} \cos(2m\pi \bar{x}) e^{-i\pi m(m+1)} e^{-\frac{i\pi}{4}} \\ &= e^{-\frac{i\pi}{4}} \psi(\bar{x}, 0); \quad m = 0, 1, 2, \dots\end{aligned}\quad (20)$$

At $t = T_{rv}/8$ the state is the same as what it was at $t = 0$ except for a constant phase factor. Thus there will be full revivals at multiples of $t = T_{rv}/8$. Similarly, for the odd parity states ($\psi(\bar{x}) = -\psi(-\bar{x})$) the contribution will only be from the first summation containing the sines. At $t = T_{rv}/4$, the time evolved state can then be written as:

$$\begin{aligned}\psi(\bar{x}, \tau) &= \sum_{n(\text{even})} \sqrt{2} e^{-2\pi i n^2 \tau} c_n \sin n\pi \bar{x} \\ &= \sum_m \sqrt{2} \sin(2m\pi \bar{x}) e^{-2\pi i m^2} \\ &= \psi(\bar{x}, 0); \quad m = 0, 1, 2, \dots\end{aligned}\quad (21)$$

Thus full revivals occur here at multiples of $t = T_{rv}/4$. For the case where the initial Gaussian has mean position $x_0 = 0.2L$ (a state which does not have a definite parity), there is a complete revival only at T_{rv} though partial revivals can be seen at multiples of $t = T_{rv}/3$ (Fig.4(c)). These symmetry features have an interesting analog in the regeneration characteristics of a field $E(x)$ of wavelength λ propagating through a multimode planar waveguide of width b [15]. If the field is symmetric in the transverse dimension ($E(x) = E(-x)$), its regeneration length is $L = b^2/\lambda$. An antisymmetric field regenerates at a distance $2L$ and arbitrary fields regenerate at a distance $2L$ and arbitrary fields reproduce after $8L$. In the case of wavepacket dynamics in square well potentials, these symmetry aspects are more clearly understood for the infinite square well potential. However, it is not surprising that we see similar features for wavepacket dynamics in the finite well analyzed here.

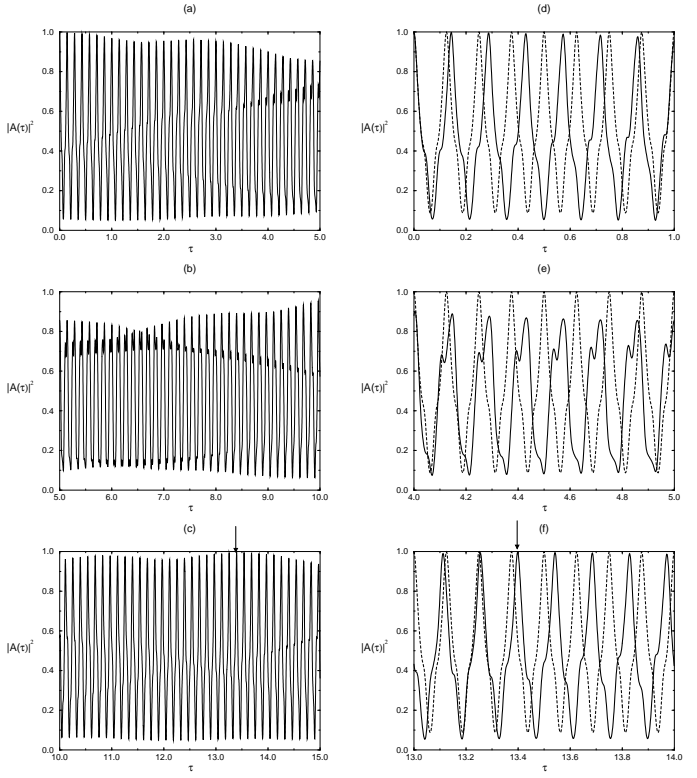


FIG. 3. Square of the autocorrelation function, $|A(\tau)|^2$ vs the scaled time τ for an initial Gaussian wavepacket of width $L/10$ and with mean position at $\bar{x} = 0.0$ for $\epsilon = 15$ ($N \sim 10$). (c) and (d) highlight the detailed behaviour at shorter times and (e) highlights the detailed behaviour near the superrevival time (e) highlights the detailed behaviour near the superrevival time (e) highlights the detailed behaviour near the superrevival time. The arrow marks the first superrevival. The dashed curves correspond to the corresponding plot for the infinite square well.

Also, notice that for the initial Gaussian wavepacket centered at $x_0 = 0.0$, the autocorrelation function, $|A(\tau)|^2$ is never zero (Figs.2 and 3). On the other hand if we examine the case where $x_0 = 0.2L$ (Fig.4), there will be times when $|A(\tau)|^2$ is zero and these times normally correspond to those instants when the wavepacket appears almost as a mirror reflection of itself and hence completely uncorrelated with what it was at $t = 0$. Local extrema of the autocorrelation function, on the other hand, correspond to ‘fractional revivals’, i.e., when the wavepacket appears in a spatially separated superposition of replicas of itself (cat-like states). As mentioned before, the absence of a simple analytical form for the

energy eigenvalues for the finite well makes it difficult to find estimates for the superrevival times. The nature of these superrevivals and how often they occur would also depend on various factors like the well-strength and the initial position of the wavepacket.

Comparison with an anharmonic oscillator

As mentioned above, the lack of an analytical form for the energy makes it difficult to estimate the superrevival times for the finite well. However, to get some insight, the revival and superrevival structure in wavepacket dynamics of the finite well may be compared with the wavepacket dynamics in an anharmonic oscillator potential where one has the exact analytical expression for the energy. We examine the hamiltonian with nonvanishing third order nonlinearity:

$$H = \mu_1(a^\dagger a)^2 + \mu_2(a^\dagger a)^3. \quad (22)$$

Here a and a^\dagger correspond to the annihilation and creation operators, respectively. This system has been studied by Gantsog et al [16], though not in the context of quantum revivals. To make a comparison with the dynamics of the Gaussian wavepacket in the case of the finite well, one can study the dynamics of initial coherent states and squeezed states for the system described by (19). We assume that $\mu_2 \ll \mu_1$. It can be easily checked that the revival times and superrevival times for the system (19) are given by:

$$t'_{rv} = \frac{t_{rv}}{(1 + 3\bar{n}\beta)}, \quad (23)$$

$$t_{sr} = t_{rv}/\beta,$$

where $t_{rv} = \frac{2\pi\hbar}{\mu_1}$, is the revival time without the third order term, i.e., with $\mu_2 = 0$ and $\beta = \frac{\mu_2}{\mu_1}$. \bar{n} is the average photon number corresponding to the chosen initial state. Initial coherent and squeezed states can be expressed in terms of the Fock states, $|n\rangle$, and one can study their time evolution. The autocorrelation for an initial coherent state with amplitude α can be easily shown to be

$$|A(\tau)|^2 = \left| \sum_n \frac{|\alpha|^n e^{-\frac{|\alpha|^2}{2}}}{n!} \exp\left(-2\pi i \tau n^2 - 2\pi i \beta \tau n^3\right) \right|^2, \quad (24)$$

while for an initial squeezed state, the autocorrelation function is given by

$$|A(\tau)|^2 = \left| \sum_n \frac{2\sqrt{s}}{(s+1)2^n n!} \left(\frac{s-1}{s+1}\right)^n H_n^2\left(\frac{s\sqrt{2}\alpha}{\sqrt{s^2-1}}\right) \exp\left(-\frac{2s\alpha^2}{s+1} - 2\pi i \tau n^2 - 2\pi i \beta \tau n^3\right) \right|^2. \quad (25)$$

Here H_n denotes the n th order Hermite polynomial, s is the squeeze parameter [17] and $\tau = t/t_{rv}$ is the scaled

time. Although the system described by (19) is not quite the same as the finite well potential, one sees certain similarities in the autocorrelation function in both cases.

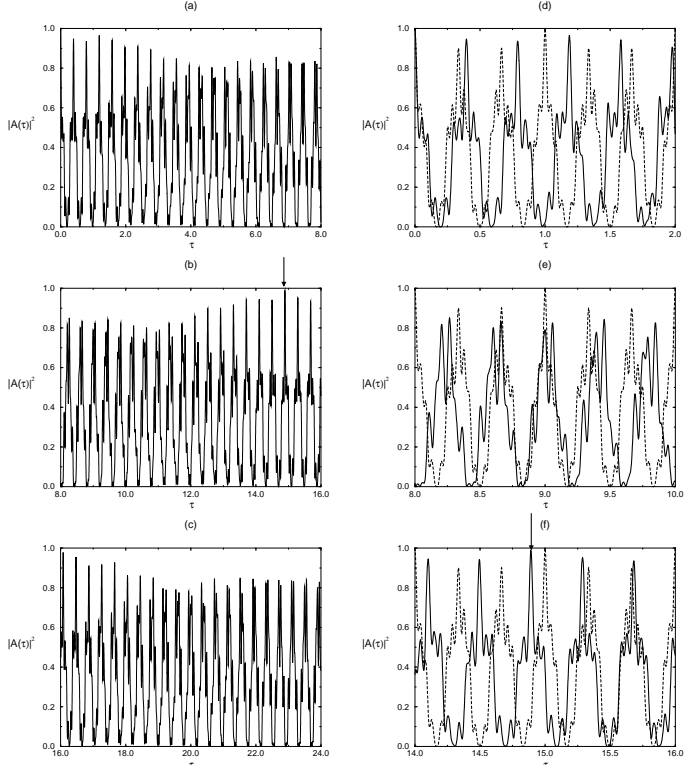


FIG. 4. Square of the autocorrelation function, $|A(\tau)|^2$ vs the scaled time τ for an initial Gaussian wavepacket of width $L/10$ and with mean position at $\bar{x} = 0.2L$ for $\epsilon = 12$ ($N \sim 8$). (c) and (d) highlight the detailed behaviour at shorter times and (e) highlights the detailed behaviour near the superrevival time (e) highlights the detailed behaviour near the superrevival time. The arrow marks the first superrevival. The dashed curves correspond to the corresponding plot for the infinite square well.

The time evolution of an initial squeezed vacuum state ($\alpha = 0$) in the anharmonic oscillator potential (19) can be compared with that of the narrow Gaussian wavepacket centered at $x_0 = 0.0$ in the finite quantum well. Fig. 5 shows the autocorrelation function for the dynamics of an initial squeezed vacuum in the the anharmonic potential (19) with squeeze parameter $s = 10$, and $\beta = .002$ for short times as well as for times close to the superrevival times. In both these cases one can see that the autocorrelation functions never go to zero unlike the case when $x_0 \neq 0.0$ for the packet in the finite potential well and $\alpha \neq 0$ for the coherent state/squeezed state

in the anharmonic potential (results not shown for the anharmonic oscillator model). For this ‘symmetric case’, there are many more revivals at short times and superrevivals at longer times in both cases in contrast with the case when $x_0 \neq 0.0$ and $\alpha \neq 0$ when there are fewer revivals and superrevivals. For the anharmonic oscillator the autocorrelation function also indicates the presence of fractional superrevivals as seen in the finite well potential. In particular one can compare the signature of the occurrence of superrevivals in both potentials by comparing the detailed structure of the autocorrelation functions at times close to the superrevivals times. In both cases one can see that at times nearing the superrevival times, the autocorrelation function begins to look more and more like the behaviour near $\tau = 0$ and near the revivals times. Moreover, at exactly these superrevival times the form of the autocorrelation function for the finite well appears very similar to that of the infinite well and in the corresponding case for the oscillator, the autocorrelation function at these times resembles the behaviour for the case when $\mu_2 = 0$. At all other times away from the revival and superrevival times, the autocorrelation functions look very different. This is clear from Figs. 2, 3 and 4 where the detailed behaviour of the autocorrelation function for the well at short times and near the superrevivals times are highlighted. Thus the gross features regarding the nature of revivals and superrevivals of wavepackets in the finite potential well are quite comparable with the dynamics of coherent potential well are quite comparable with the dynamics of coherent and squeezed states in a generic anharmonic oscillator potential (19).

IV. CONCLUSION

In conclusion, we have studied the wavepacket dynamics in a finite square well potential in the context of quantum revivals. We have shown that for short times the revival patterns are similar to that seen in the infinite well potentials but with a modified revival time which is now dependent on the depth of the finite well. For deep enough wells, the time scales approach closer to that of the infinite well. For longer times, the difference in the wavepacket dynamics as compared to the infinite well potential is manifested by the appearance of superrevivals. Superrevivals have till now been predicted for the long time dynamics of Rydberg wavepackets [9].

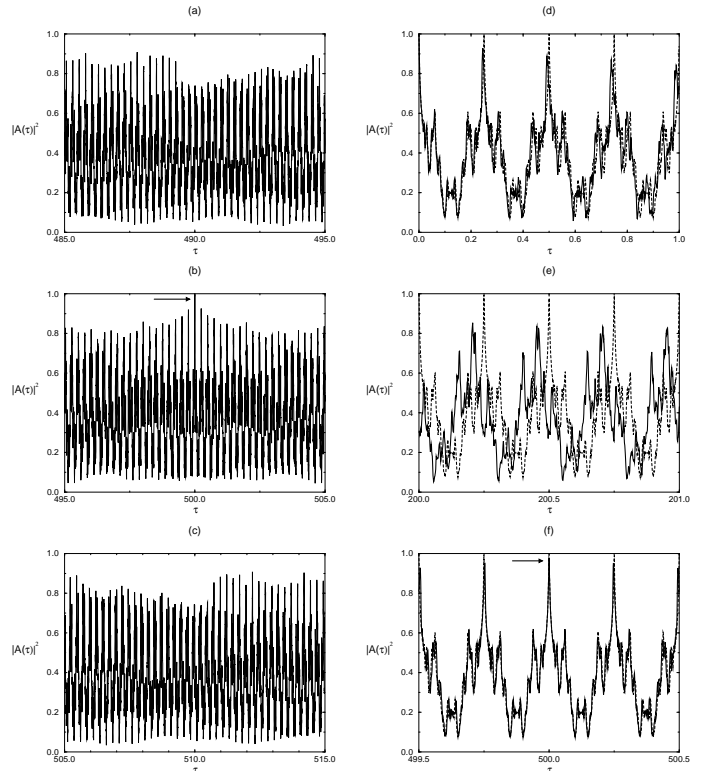


FIG. 5. **Square of the autocorrelation function, $|A(\tau)|^2$ vs the scaled time τ , ($\tau = t/t_{rv}, t_{rv} = 2\pi\hbar/\mu_1$) for an initial squeezed vacuum with squeeze parameter $s = 10$ and $\beta = .002$ for the anharmonic oscillator potential (19). (c) and (d) highlight the detailed behaviour at shorter times and (e) highlights the detailed behaviour near the superrevival time, $T_{sr} = T_{rv}/\beta = 500T_{rv}$. The arrow marks the first superrevival. The dashed curves correspond to the case when $\mu_2 = 0$**

The analysis in this paper predicts that wavepacket dynamics in quantum well systems which can be more realistically modelled as finite square well potentials rather than infinite ones, will show superrevivals in addition to the usual revivals.

One of us (GSA) is grateful to W. Schleich for useful discussions on the dynamics of wavepackets.

[†] E-mail address:anu@prl.ernet.in

[‡] E-mail address:gsa@prl.ernet.in

- [1] J. Parker and C. R. Stroud, Phys. Rev. Lett. **56**, 716 (1986); Phys. Scr. **T12**, 70 (1986)
- [2] G. Alber, H. Ritsch and P. Zoller, Phys. Rev A **34**, 1058 (1986)
- [3] I. Sh. Averbukh and N. F. Perelman, Phys. Lett. **139A**, 449 (1989)
- [4] R. Bluhm ,V. A. Kostelecky and J. A. Porter, Am. J. Phys. **64** (7), 944 (1996)
- [5] B. M. Garraway and K-A Suominen, Rep. Prog. Physics **58**, 365 (1995); W. S. Warren, H. Rabitz and M. Dahleh, Science **259**, 1581 (1993); Marc. J. J. Vrakking, D.M. Villeneuve and Albert Stolow, Phys. Rev. A **54**, 37 (1996); I. Sh. Averbukh, Marc. J. J. Vrakking, D.M. Villeneuve and Albert Stolow, Phys. Rev Lett. **77**, 3518 (1997).
- [6] K. Leo, J. Shah and E. O. Gobel, Phys. Rev. Lett. **66**, 201 (1991)
- [7] G. Rempe, H. Walther and N. Klein, Phys. Rev. Lett. **58**, 353 (1987); I. Sh. Averbukh, Phys. Rev. A **46**, R2205 (1992)
- [8] D. M. Meekhof, C. Monroe, B. E. King, W. M. Itano and D. J. Wineland, Phys. Rev. Lett. **76**, 1796 (1996).
- [9] R. Bluhm and V. A. Kostelecky, Phys. Rev A **50**, R4445 (1994); R. Bluhm and V. A. Kostelecky, Phys. Lett. 200 A, **308** (1995)
- [10] D. L. Aronstein and C. R. Stroud, Phys. Rev. A **55** (6), 4526 (1997)
- [11] M. V. Berry, J. Phys. A **29**, 6617 (1996); M. V. Berry and S. Klein, J. Mod. Optics **43**, 2139 (1996)
- [12] F. Gossiβmann, J-M Rost and W. P. Schleich, J.Phys. A Gen **30**, L277 (1997); P. Stifter, C. Leichtle, W.P. Schleich and J. Marklof, Z. Naturf. **52**, 377 (1997); P. Stifter, W. E. Lamb, Jr and W. P. Schleich in *Frontiers of Quantum Optics and Laser Physics*, Eds. S. Y. Zhu, M. S. Zubairy and M. O Scully (Springer, Singapore 1997), p 236
- [13] A. M. Weiner, J. Opt. Soc. Am. B **11**, 2480 (1994)
- [14] B. I. Barker, G. H. Rayborn, J. W. Ioup and G.E. Ioup, Am. J. Phys. **59**, 1038 (1991)
- [15] J. Banerji, J. Opt. Soc. Am. B **14**, 2378 (1997); J. Banerji, A. R. Davies and R. M. Jenkins, Appl. Opt. **36**, 1604 (1997).
- [16] Ts. Gantsog and R.Tanaś, Quantum Opt. **3**, 33 (1991).
- [17] W. Schleich and J. A. Wheeler, Nature **326**, 574 (1987)